



Research article

Enoxaparin sodium bone cement displays local anti-inflammatory effects by regulating the expression of IL-6 and TNF- α

Kangning Hao^a, Linchao Sang^a, Luobin Ding^a, Xiaoyu Shen^a, Dehao Fu^b,
Xiangbei Qi^{a,*}

^a Department of Orthopaedic Surgery, The Third Hospital of Hebei Medical University, 139#Ziqiang Road, Shijiazhuang, Hebei Province, China

^b Department of Orthopedics, Shanghai General Hospital, Shanghai Jiao Tong University School of Medicine, Shanghai, China

ARTICLE INFO

Keywords:

Interleukin-6
Tumour necrosis factor- α
Pathology
Cell apoptosis
Inflammation

ABSTRACT

Objective: To explore the roles of Enoxaparin Sodium-Polymethyl methacrylate bone cement on inflammatory factors Interleukin-6 and Tumour Necrosis Factor- α in a rabbit knee replacement model. As well as the mechanisms underlying its potential effects on lipopolysaccharide-induced endothelial cell injury.

Methods: A knee replacement model was established using New Zealand rabbits. Forty rabbits were randomly divided into four groups: PMMA, ES-PMMA, sham-operated, and blank control groups (n = 10 in each group). Local tissues around the incision were taken at the 30th, 60th, and 90th minute after the surgical implantation of the corresponding bone cement. Immunohistochemistry in the surgical field was used to measure the expression of local inflammatory factors IL-6 and TNF- α . In the in vitro experiments, 1 cm³ of bone cement was immersed in 3 mL of the medium for 24 h. The bone cement was discarded and diluted to 25% with normal medium. Pre-experiments were screened for the best LPS-inducing concentration of 100 mg/mL, and the most compatible LPS concentration was used for subsequent experiments simulating the primary cultures of rats' Inferior Vena Cava Endothelial Cells. The experiments were divided into four groups: blank control group, LPS induction group, PMMA + LPS group, and ES-PMMA + LPS group. The apoptosis rate was detected by flow cytometry, and the expression levels of TNF- α and IL-6 in the cells and supernatant were measured by ELISA, western blotting, and immunofluorescence.

Results: According to immunohistochemical results, IL-6-positive cells were concentrated in the tissue interstitial space. In the PMMA and sham-operated groups, the number of IL-6-positive cells gradually increased over time. At all time points, IL-6 expression in the ES-PMMA group was much lower than in the PMMA and sham-operated groups. At 30 min, TNF- α positive cells in the ES-PMMA group expressed less than those in the PMMA and sham-operated groups, with no discernible difference between the PMMA and ES-PMMA groups at 60 or 90 min. Using ELISA and flow cytometry, the expression levels of IL-6 and TNF- α were improved and the apoptosis rate was magnified in the LPS-induced group (***P* < 0.001) in contrast with the blank control group. Additionally, the expression levels of IL-6 and TNF- α were reduced in the ES-PMMA + LPS group compared with the LPS-induced group (**P* < 0.05) and the apoptosis rate was reduced (***P* < 0.001), with statistically significant variations. Western blotting and immunofluorescence

Abbreviations: ES, enoxaparin sodium; PMMA, polymethylmethacrylate; ES-PMMA, enoxaparin sodium-polymethylmethacrylate; LPS, lipopolysaccharide; EC, endothelial cell; IL-6, interleukin-6; TNF- α , tumour necrosis factor- α .

* Corresponding author. Department of Orthopaedic Surgery, The Third Hospital of Hebei Medical University, Shijiazhuang, China.

E-mail address: qixiangbei2022@163.com (X. Qi).

<https://doi.org/10.1016/j.heliyon.2023.e16530>

Received 2 March 2023; Received in revised form 10 May 2023; Accepted 19 May 2023

Available online 25 May 2023

2405-8440/© 2023 The Authors. Published by Elsevier Ltd. This is an open access article under the CC BY-NC-ND license (<http://creativecommons.org/licenses/by-nc-nd/4.0/>).

analysis confirmed that IL-6 and TNF- α protein expression in cells was upregulated in the LPS-induced group compared to the blank control group ($***P < 0.001$), and the mean fluorescence intensity was enlarged ($***P < 0.001$). Meanwhile, IL-6 and TNF- α expression in the ES-PMMA + LPS group were down-regulated ($**P < 0.01$ or $*P < 0.05$) compared with the LPS-induced group and PMMA + LPS group protein expression, and the average fluorescence intensity of IL-6 and TNF- α was lowered in the ES-PMMA + LPS group compared to the LPS-induced group ($***P < 0.001$).

Conclusions: ES-PMMA bone cement reduced the expression levels of local inflammatory factors IL-6 and TNF- α in a rabbit knee model. ES-PMMA bone cement reduced the rate of LPS-induced endothelial cell apoptosis and diminished local inflammatory damage by regulating the secretion of inflammatory factors TNF- α and IL-6.

1. Introduction

Polymethyl methacrylate (PMMA) bone cement is an essential material commonly used as a filler and stabilizing agent in knee arthroplasty to fasten the prosthesis to bone tissue during surgery [1,2]. However, intraoperative bone cement implantation can lead to several complications, including decreased blood pressure, respiratory distress, deep vein thrombosis, and even pulmonary embolism, collectively known as bone cement implantation syndrome (BCIS) [3,4]. Recent studies on BCIS have found that the polymerisation reaction during bone-cement implantation releases large amounts of heat. The physical and chemical stimulation of local tissues during the reaction can damage the vascular endothelium, activate the body's coagulation system, form microthrombi, and block small pulmonary arteries [5]. Simultaneously, local vascular endothelial injury releases inflammatory factors, which alter the local inflammatory microenvironment and exacerbate injury. Additionally, prophylactic systemic anticoagulation is usually suspended during the perioperative period of knee arthroplasty to reduce the bleeding risk. Paradoxically, however, the withdrawal of anticoagulation therapy increases the risk of thromboembolism. Although antibiotic-loaded bone cement has been clinically effective in knee replacement surgery, it has not been found to reduce thrombosis during this period. Therefore, knee replacement surgery must address the need to prevent thrombosis and reduce the local inflammatory responses during this period.

Previous studies have demonstrated that enoxaparin sodium can be released from solidified PMMA bone cement and can tolerate the released heat, retaining its anticoagulant activity, reducing thrombosis, and producing a local anticoagulant effect by modulating endothelial CD40 levels [6,7]. Moreover, in a recent study, we found that the addition of alendronate to ES-PMMA bone cement promoted the repair of tibial bone defects, which represents a significant advantage [8]. Studies have reported that the release of various inflammatory mediators, such as IL-1 β and TNF- α , can be induced after knee replacement surgery [9]. Notably, inflammatory factors also play a central role in thrombosis [10]. In addition to its anticoagulant effect, low-molecular-weight heparin inhibits IL-6 and TNF-induced inflammation [11]. Inflammation can trigger thrombosis, and thrombosis can further exacerbate the development of inflammation. This vicious circle is known as the "thrombotic-inflammatory response" [12]. Studies have shown a significant link between IL-6 and TNF- α and thrombosis [13], hence the selection of these two inflammatory factors in our study.

However, few studies have reported whether ES can reduce the expression of inflammatory factors and alter the local inflammatory microenvironment, thereby reducing complications arising from EC damage throughout the knee replacement procedure. In the present study, we exploited the good release properties of ES-PMMA bone cement and described the local anti-inflammatory effect of this novel material. This study provides theoretical data for future research on the molecular mechanisms underlying its anti-inflammatory effects.

2. Materials and methods

2.1. Preparation of bone cement specimens

PMMA bone cement (Palacos® R; Heraeus Medical GmbH, Germany, 40 g/pack) and ES powder (8000 AXaIU; Chengdu Bai Yu Pharmaceutical Co. Ltd.) were blended as previously described at 23 ± 1 °C [6]. Before the experiment, the mixed ES-PMMA bone cement powder and PMMA powder were introduced into the liquid phase. The two types of bone cements were mixed evenly to prepare $1 \times 1 \times 1$ -cm specimens, which were autoclaved before use.

2.2. Animal models and groups

Forty adult New Zealand rabbits of either sex (4–6 months old, mean weight 2.8 kg) were selected for all in vivo experiments (animal certificate no. 210509; Wangdu Tong Hui Animal Breeding Co. Ltd.). The animal experiment protocol was approved by the Medical Ethics Committee of the Third Hospital of Hebei Medical University (approval no. z2021-007-2). The femoral condyle prosthesis and tibial plateau prosthesis are two components of the rabbit knee prosthesis. The structure and dimensions of the prosthesis were designed and made precisely according to the biological and anatomical characteristics of the rabbit knee joint with modifications to ensure an intraoperative match with the reference [14,15]. The rabbits were randomly divided into four groups of ten animals: sham-operated group, blank control group (control), PMMA group, and ES-PMMA group. The animals were fasted preoperatively with water for 4 h, and pentobarbital sodium 30 mg/kg was administered intravenously via the ear margins to ensure that

the rabbits were unconscious during the operation. The surgical procedures were conducted by the same team. The surgical processes of the four groups are briefly described as follows: The hair in the surgical area was trimmed, routine disinfection was performed, and sterile drapes were placed. The medial parapatellar incision was approximately 5 cm long, and the joint capsule was incised through it. The patella was drawn laterally to expose the joint cavity, the knee was flexed at 90°, and the tibial plateau was fully exposed. The anterior cruciate ligament of the knee was cut and the medial and lateral menisci were removed. The bone surface of the tibial plateau was truncated by 2 mm and the femoral condyle was regularly truncated according to the prosthesis standard with a thickness of 2 mm. Subsequently, the femoral and tibial medullary cavities were drilled and reamed to depths greater than 15 and 10 mm, respectively. Subsequently, the joint cavity was washed with 0.9% saline and the prosthesis was placed on a trial basis. The prosthesis was removed and the two prepared bone types of cement were mixed with the liquid-phase monomer; 3 mL was applied around the prosthesis during the dough phase and injected into the medullary cavity with a syringe, followed by the placement of the prosthesis in complete contact with the osteotomy surface. To avoid interference from other factors, the surgical wound was covered with a sterile dressing before sample collection, and the incision was closed after sample collection. No antibiotics were administered postoperatively to prevent infection and the principle of asepsis was followed during the experiments.

2.3. Sample collection

Tissue samples from the PMMA and ES-PMMA groups were taken at 30, 60, and 90 min after bone cement implantation from the surrounding adhesion-stained bone cement, while the same sample sites were taken at the corresponding time points in the sham-operated and control groups.

2.4. Immunohistochemical

Recombinant *anti*-IL-6 antibody (Abcam) and *anti*-TNF- α antibody (Abcam) were used as primary antibodies and horseradish peroxidase (HRP)-labeled sheep anti-rabbit IgG (Abcam) was used as the secondary antibody. 3,3-diaminobenzidine (DAB) (Zhongshan Jin Qiao, Beijing, China) was used as a chromogen. Tissue samples were fixed in 4% paraformaldehyde (PFA) for 24 h and then paraffin-embedded before transferring into the melted paraffin solution for about 3 h. Next, drops of polylysine working solution (1:10 dilution) were placed on coverslips at 500 μ L/slice, pushed, and dried naturally. The primary antibody was added dropwise and incubated overnight at 4 °C for 1 h. Then, the slices were washed three times with PBS for 5 min. The secondary antibody was added dropwise and the mixture was incubated for 20 min at room temperature. DAB was used as the chromogen, and haematoxylin was used as the counterstain. Lastly, the sections were photographed under a microscope ($\times 200$ magnification).

2.5. Cell culture and MTT assay

Primary cultures of rats' Inferior Vena Cava Endothelial Cells in DMEM (Gibco, USA) medium (10% fetal bovine serum, Gibco, USA). Cells were incubated in a 37 °C, 5% CO₂, saturated humidity incubator. When they reached 80%–90% confluence, cells were passaged. Rat endothelial cells (Hunan Feng Hui Biotechnology Co. Ltd. China) were treated with 0 mg/mL, 50 mg/mL, 100 mg/mL, and 150 mg/mL of LPS respectively for 48 h. They were inoculated into 96-well plates with 3000 cells/well. Treatment of rat endothelial cells with 100 mg/mL of LPS for administered time (0 h, 24 h, 48 h, 72 h).

Briefly, 10 μ l of MTT (Ameresco, USA) solution (10 mg/mL) was added to each well, followed by incubation at 37 °C for 4 h. Carefully aspirate the original culture solution, then DMSO (100 μ l) was added to each well to dissolve the formazan crystals. The absorbance was measured at 490 nm and evaluated.

2.6. Flow cytometry

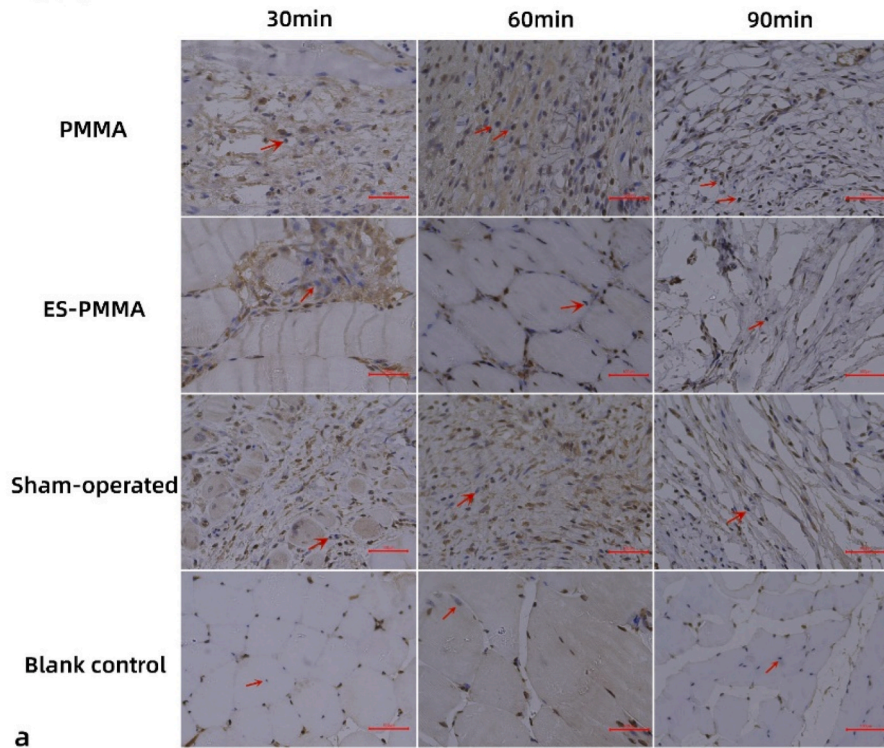
The cells were divided into four groups: blank (control), LPS, PMMA + LPS, and ES-PMMA + LPS. The primary cultures of rat inferior vena cava endothelial cells were obtained from Hunan Feng Hui Biotechnology Co. Ltd. (China) and used in experiments during passages 2–3. The cells were cultured in a 5% CO₂-saturated humidity incubator at 37 °C.

Cells in logarithmic growth phase were subjected to tryptic digestion (Solabao Technology Co., Ltd. China) and then inoculated in a 6-well plate. Treatments were administered following the above groupings, and the cells were cultured for an additional 24 h. Approximately 5×10^4 to 1×10^5 cells were collected and resuspended in binding buffer from the Annexin V-FITC kit (Hangzhou Unitech Biotechnology Co. Ltd., China). Next, 5 μ l of Annexin V-FITC and 10 μ l of propidium iodide (PI) solution were added. The cells were then further incubated at room temperature (20–25 °C) in the dark for 10–20 min and placed in an ice bath. Data were acquired using a FACS Calibur™ flow cytometer (BD Biosciences).

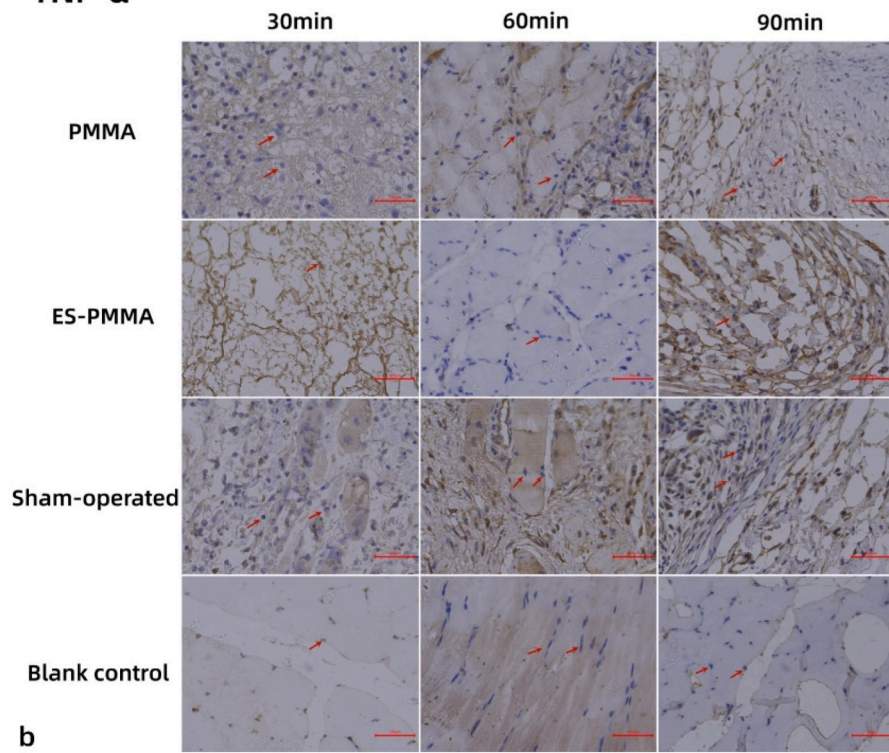
2.7. ELISA assay

The main reagents for the cell experiments were rat interleukin 6 (IL-6) ELISA kit (Elite, Wuhan, China) and rat tumour necrosis factor- α (TNF- α) ELISA kit (Elite, Wuhan, China). The cells were grouped as in flow cytometry assay. The culture supernatant of the 2–3 generation cells was collected and centrifuged for 20 min to remove impurities and debris. Subsequently, 100 μ l of sample and standard was added per well and incubated for 1.5 h at 37 °C. After removing the liquid but not washing, 100 μ l of Biotin-antibody was added to each well and then incubated at 37 °C for 1 h. An enzyme conjugate working solution of 100 μ l was added, and the plate was

IL-6



TNF- α



(caption on next page)

Fig. 1. Effect of ES-PMMA on the expression of surgical local inflammatory factors in rabbits.

(a, b) IL-6 and TNF- α expression in local tissue samples from the surgical area of each group at 30, 60, and 90 min. Red arrows indicate positive stained cells ($\times 200$ magnification). (For interpretation of the references to colour in this figure legend, the reader is referred to the Web version of this article.)

placed in an incubator at 37 °C for 30 min. After washing, TMB substrate was added to each well and incubated in the dark for 15 min. The reaction was stopped by adding a termination solution directly to each well. Lastly, the optical density (OD) was measured at a wavelength of 450 nm.

2.8. Western blotting

The original culture medium of each group of cells was aspirated and discarded, and the protein content was determined using the BCA method. Cells were grouped as described above. The original culture medium of each group of cells was aspirated and discarded. After washing once with 1 \times PBS, RIPA (Solebro Technology Ltd, China) 1000 μ L/well was added. Then shaking at 4 °C for 30 min, transfer the cell lysate to a 1.5 mL centrifuge tube to obtain a cell protein sample. The protein concentration was calculated based on the standard curve of BSA. Protein concentration of samples was calculated using a Bradford assay. Protein samples were resolved by sodium dodecyl sulfate-polyacrylamide gel electrophoresis and transferred to PVDF (Millipore, USA). The primary antibodies anti-TNF- α antibody (Abcam, UK) and anti-IL-6 antibody (Abcam, UK) (1:1000) were added to the incubation kit at 4 °C overnight under shaking. The membranes were placed in 1 \times TBST solution and rinsed four times for 5 min with shaking four times. The membranes were incubated with HRP-labeled secondary antibody (goat anti-rabbit IgG; Abcam, UK) (1:8000) of the corresponding species origin for 1.5 h at room temperature and washed with TBST solution four times for 5 min each. Color development was performed using ECL chemiluminescent reagents. Western blotting protein markers were obtained from Solebro Technology Ltd. (Beijing, China). Western blot analysis was performed using GAPDH antibody (Abcam, Cambridge, UK). Lastly, the films were scanned and imaged using an Epson Perfection V39 scanner, and the brightness values of the protein bands were analyzed.

2.9. Immunofluorescence

Cells were seeded in 24-well plates overnight, treated according to the experimental groups, and aspirated, followed by the addition of 1 mL of 4% paraformaldehyde fixative. Closure solution was used for 60 min, and the solution was removed and diluted with primary anti-TNF- α (TNF- α monoclonal antibody; Protein Tech, USA) (1:50) and IL-6 (anti-IL6 antibody produced in rabbit Item, Sigma, Germany) (1:50) overnight at 4 °C. The primary antibody was removed, and the cells were washed three times with PBS for 10 min each. Fluorescence-labeled secondary antibody (goat anti-mouse IgG H&L; Abcam, UK) was added and incubated at 37 °C for 1 h. Fluorescence analysis was performed using ImageJ software.

2.10. Data analysis

Data were processed using GraphPad 6. One-way analysis of variance (ANOVA) was used for multiple comparisons between groups, and measurement data were expressed as mean \pm standard deviation (SD). Differences were considered statistically significant at $P < 0.05$.

3. Results

3.1. Local IL-6 and TNF- α expression was detected at distinct time intervals in rabbit models

The immunohistochemical results of the four groups were compared, and cytokine-positive cells were assessed by a senior pathologist using three high-power, non-overlapping fields on a single microscope. Positive cells stained yellowish-brown. No significant change was observed in the expression levels of IL-6 cells in the ES-PMMA group at each time point, and almost no positive cells were expressed, whereas the expression level of positive cells in the PMMA and sham-operated groups was found to increase with time (Fig. 1a). The level of TNF- α expression in the ES-PMMA group showed fewer positive cells in the field of view at each period than in the PMMA and sham-operated groups. This indicated that ES-PMMA bone cement can reduce IL-6 and TNF- α expression in the local surgical area (Fig. 1b).

3.2. Optimal induction concentration of LPS and inhibition of LPS-induced apoptosis in endothelial cells by ES-PMMA in vitro

In the preliminary experiments, we stimulated rat endothelial cells with different concentrations (0, 25, 50, 100, and 150 mg/mL) of LPS, and the MTT (3-(4,5-dimethylthiazol-2-yl)-2,5-diphenyltetrazolium bromide) method was used to screen LPS concentrations in different subgroups. The optimal induction concentration of LPS on rat endothelial cells was 100 mg/mL, with a maximum cell survival rate of 80% at 24 h. The cell survival rate decreased significantly with time (Fig. 2a). Therefore, we chose 100 mg/ml as the optimal experimental induction concentration. The results of flow cytometry analysis demonstrated that the apoptosis rate was increased in the LPS-induced group compared to the blank control group ($***P < 0.001$) and decreased in the ES-PMMA + LPS group compared to the

LPS-induced group ($***P < 0.001$), with statistically significant differences (Fig. 2b).

3.3. Secretion of inflammatory factors IL-6 and TNF- α in vitro in cell cultures were measured by ELISA

We detected the expression of IL-6 and TNF- α in the cell culture supernatant using ELISA, and found that IL-6 and TNF- α expression was significantly higher in the LPS-induced than in the blank control group ($***P < 0.001$), whereas expression in the ES-PMMA + LPS group was lower than that in the LPS-induced group ($*P < 0.05$) (Fig. 3).

3.4. Protein expression of IL-6 and TNF- α in cell cultures was determined by western blotting

Western blot assays showed that endothelial cells secreted IL-6 and TNF- α proteins after lysis. The expression of IL-6 and TNF- α was elevated in the LPS-induced group compared with the blank control group ($***P < 0.001$), while the expression of both proteins was reduced in the ES-PMMA + LPS group compared with the LPS-induced and PMMA + LPS groups $P < 0.05$ or $**P < 0.01$). In comparison, the ES-PMMA bone cement was found to inhibit IL-6 and TNF- α protein expression in endothelial cells (Fig. 4).

3.5. Immunofluorescence detection of IL-6 and TNF- α protein expression in endothelial cells in vitro

The immunofluorescence results of endothelial cells expressing IL-6 and TNF- α showed that IL-6 and TNF- α were released after cell destruction, and the mean fluorescence intensity of IL-6 and TNF- α increased in the LPS-induced group compared to the blank control group ($***P < 0.001$) and decreased in the ES-PMMA + LPS group compared to the LPS-induced group ($***P < 0.001$) ($\times 200$ magnification) (Fig. 5 a,b).

4. Discussion

Inflammation is a complex defense response to endogenous and exogenous injury factors, wherein the vascular response is central to inflammation. Under normal physiological conditions, the anti-inflammatory and pro-inflammatory elements are in equilibrium. Orthopaedic surgery, such as joint replacement surgery, can result in cyclooxygenase-2 (COX-2) expression and prostaglandin release, activating prostaglandin receptors, which expands the sensitivity of cyclic adenosine monophosphate in inflammatory cells, thereby increasing the expression of pro-inflammatory factors, such as IL-6 and TNF- α , and triggering an inflammatory response.

Studies have shown that inflammatory modifications can appear in the acute section after a joint replacement surgical procedure [16], inducing the release of inflammatory factors, inclusive of TNF- α , IL-6, IL-8, and IL-1 β , which are both transduction and effector

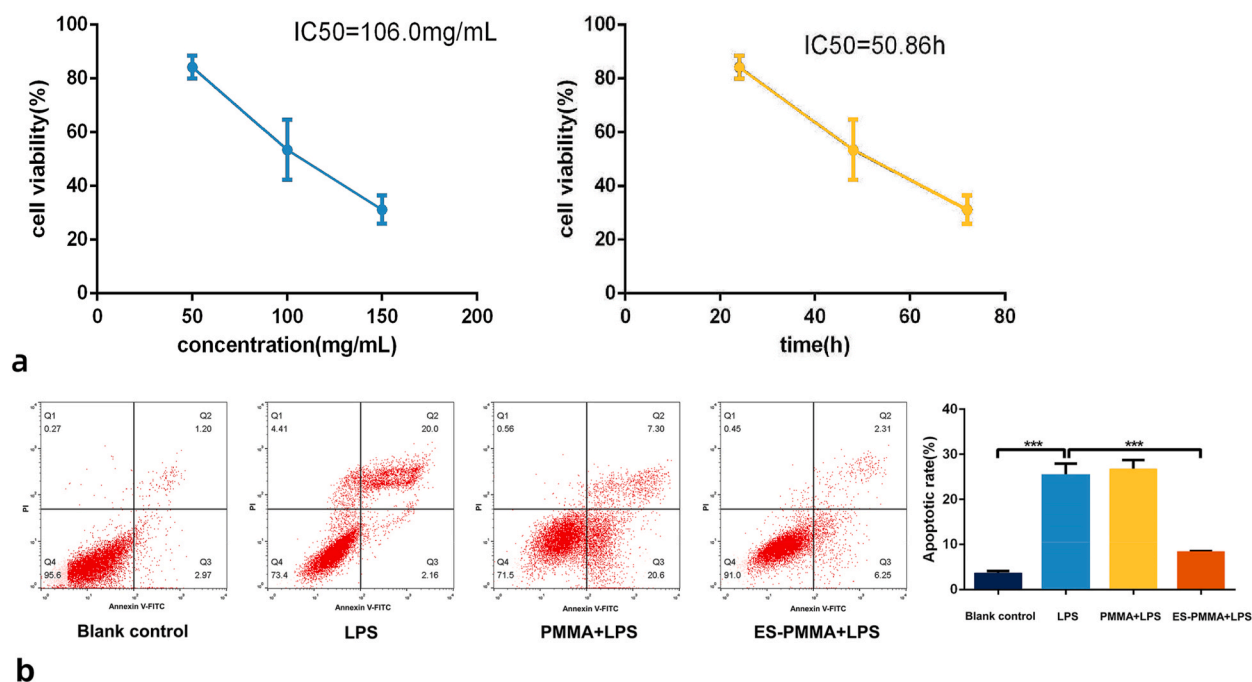


Fig. 2. Optimal induction concentration of LPS and the effect of ES-PMMA bone cement on endothelial cell apoptosis in vitro.

(a) MTT method for screening the temporal and quantitative effects of LPS in vitro.

(b) The apoptosis rate of ECs in each culture group was significantly higher in the LPS group than in the blank control group ($***P < 0.001$) and significantly lower in the ES-PMMA group than in the LPS-induced group ($***P < 0.001$) ($n = 3$).

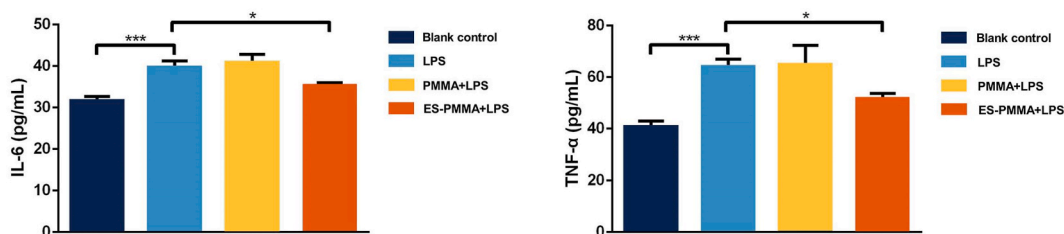


Fig. 3. ES-PMMA reduces the expression of inflammatory factors *in vitro*.

In vitro, IL-6 and TNF- α expression was significantly higher in the cell culture medium in the LPS-induced compared to the blank control group ($***P < 0.001$) but was decreased in the ES-PMMA + LPS group compared to the LPS-induced group ($*P < 0.05$) ($n = 3$).

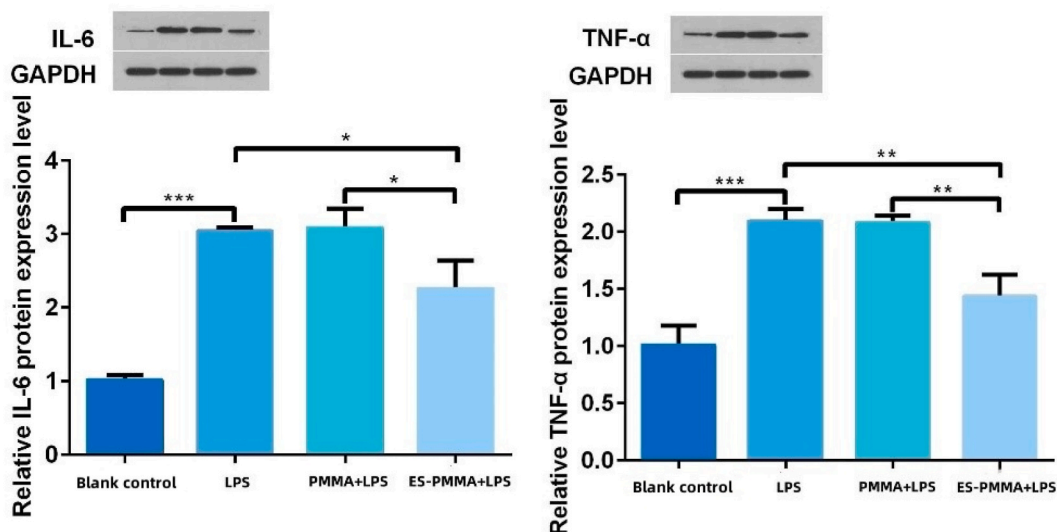


Fig. 4. ES-PMMA bone cement reduces the expression of inflammatory factors in cultures via the release of sodium enoxaparin.

The *in vitro* IL-6 and TNF- α protein expression in endothelial cells was determined by western blotting. GAPDH was used as an internal reference. IL-6 and TNF- α expression was increased in the LPS-induced group compared to the blank control group ($***P < 0.001$). IL-6 and TNF- α were decreased in the ES-PMMA + LPS group compared to both the LPS-induced and PMMA + LPS groups ($*P < 0.05$ or $**P < 0.01$) ($n = 3$).

molecules [17]]. Knee replacement surgical treatment is complex and painful. In this context, the body's inflammatory response can increase due to stress, particularly the degree of inflammatory factors, such as IL-6 and TNF- α [9]]. Most patients who undergo knee replacement surgery are already in an inflammatory state triggered by the altered pathophysiology of osteoarthritis. Surgical treatment is an invasive process with a concomitant stress response that consists of the release of inflammatory factors [18]]. The degree of the inflammatory response to a surgical operation is associated with the type of surgery. Research has shown that joint replacement surgery can result in an extensive inflammatory response [19]], which is exacerbated by bone cement.

Many pathological changes can occur in the presence of proinflammatory factors, such as altered hemodynamics, endothelial cell damage, apoptosis, platelet adhesion, aggregation and release, and thrombosis. In addition, this promotes the release of inflammatory elements and increases the degree of the inflammatory response. In recent years, the anti-inflammatory role of low-molecular-weight heparin has been widely studied. As a result, low molecular heparin has been found to enhance the inflammatory state of acute sinusitis in rats by way of inhibiting the TLR4-MyD88-NF- κ B signalling pathway [20]]. Additionally, Sollier et al. concluded that low-molecular-weight heparin exerts various activities, one of which involves an inflammatory response [21]].

Enoxaparin sodium is frequently used in clinical practice as an anticoagulant. Our previous findings confirmed that, when mixed with polymethacrylate bone cement, enoxaparin sodium can effectively release and maintain drug activity, does not participate in the polymerisation of PMMA bone cement, and resists the release of heat. It also exerts a local antithrombotic effect by modulating the expression of CD40 in endothelial cells [6,7]]. In a recent study, we found that enoxaparin sodium bone cement, to which alendronate was added, was superior to enoxaparin sodium bone cement, and PMMA bone cement in promoting the repair of tibial bone defects [8]]. This was closely related to the potency of enoxaparin sodium. However, previous studies had not taken into account the anti-inflammatory effects of enoxaparin sodium.

In the animal model used in this study, the expression of inflammatory factors increased at 30, 60, and 90 min. To rule out interference precipitated by the surgical procedure itself, a sham surgical treatment group was set up where only prosthesis implantation was performed and no cement was used. These outcomes indicated that the inflammatory response was exacerbated by the

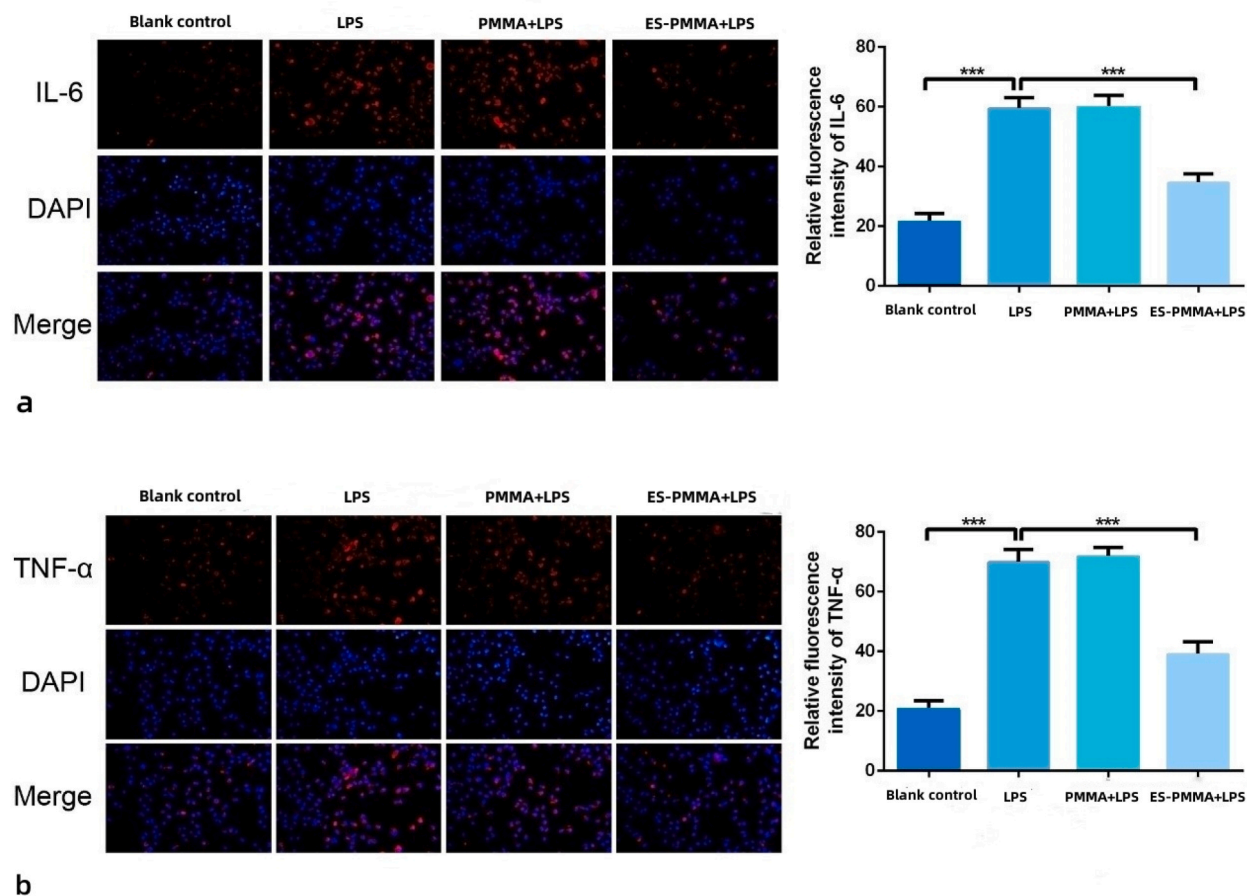


Fig. 5. ES-PMMA bone cement reduces endothelial cell inflammatory factor IL-6 and TNF- α expression via the release of enoxaparin sodium. (a, b) Expression of IL-6 and TNF- α protein in each cell group. The mean fluorescence intensity of IL-6 and TNF- α increased in the LPS-treated group compared to the blank control group ($***P < 0.001$). The mean fluorescence intensity of IL-6 and TNF- α decreased in the ES-PMMA + LPS group compared to the LPS-treated group ($***P < 0.001$) ($\times 200$ magnification).

stimulation of the surgery itself, combined with the exothermic polymerisation of the PMMA bone cement after implantation. This is consistent with results reported in the literature. In contrast, the use of ES-PMMA bone cement reduced the local inflammatory response by inhibiting the secretion of inflammatory factors IL-6 and TNF- α .

As previously mentioned, knee replacement surgical procedures can increase the expression of inflammatory factors IL-6 and TNF- α [[9]]. Thus, to explain the anti-inflammatory mechanism of ES-PMMA, *in vitro* experiments were performed. The position of inflammatory factors has been addressed in several disciplines. For example, Jeongyoon et al. [[22]] used human fibroblasts and a mouse mannequin of pores and skin infection to illustrate that Siberian alder extracts (*Alnus Sibirica*) can alter IL-1 β , IL-8, IL-6, and TNF- α expression. Similarly, through *in vivo* and *in vitro* experiments, Eun-Nam Kim et al. [[23]] found that ginseng fruit extract (PGFE) can be used to treat periodontitis by inhibiting pro-inflammatory factors, such as TNF- α , IL-1 β , and IL-6.

IL-6 is produced by a range of cells, such as macrophages, lymphocytes, endothelial cells, and tumor cells [[24]]. Moreover, it is an inflammatory marker that induces the differentiation of B lymphocytes, promotes the proliferation of T lymphocytes, and enhances the pastime of herbal killer cells, thereby contributing to the inflammatory response. TNF- α is another common pro-inflammatory cytokine that can enhance the non-specific phagocytosis of neutrophils, promote the manufacturing of hepatic acute section proteins, and has a tumour-killing effect, mainly at the start of the inflammatory response [[25]].

IL-6 and TNF- α expression are regularly used to replicate inflammatory conditions. Valle et al. [[26]] concluded that the selective inhibition of the IL-6 transduction signalling pathway attenuates inflammation and subsequent barrier disruption in the retinal endothelium. Shirakura et al. [[27]] also found that the endothelial Robo4 receptor promotes IL-6 production through endothelial cells and immune cells via crosstalk between signalling pathways, showing that TNF- α substantially increases endothelial permeability and leukocyte recruitment, promoting inflammatory responses [[28,29]]. Additionally, Palanisamy Nallasamy et al. [[30]] concluded that the natural compound resveratrol attenuates TNF- α -induced vascular dysfunction in mice and human endothelial cell inflammatory responses, as well as enhancing cell survival and protecting mouse aortic endothelial cells (MAECs).

The nuclear transcription component κ B (nuclear element kappa B, NF- κ B) is an essential signalling pathway that mediates

inflammation. Studies have demonstrated that LPS has an activating impact on the NF- κ B signalling pathway, which leads to an inflammatory response. As a result, LPS is regularly used to artificially induce an inflammatory response [[31,32]]. In this study, we selected rat endothelial cells triggered by LPS, an endotoxin, a complex of lipids, and polysaccharides from the outer wall of Gram-negative bacteria.

As mentioned earlier, joint replacement surgery can cause local endothelial cell damage and the secretion of inflammatory factors. By detecting the expression levels of IL-6 and TNF- α in response to endothelial cell injury, the LPS-induced and PMMA + LPS-induced groups were found to express IL-6 and TNF- α to various degrees, combined with an increased apoptosis rate, whereas the ES-PMMA + LPS-induced group showed both decreased inflammatory factor expression and apoptosis rate. This further explains the results of the animal studies and suggests that ES-PMMA bone cement can inhibit the initiation of inflammatory factors, alter the local inflammatory microenvironment during surgery, and exert anti-inflammatory effects.

This study has some limitations. The inflammatory response is a complicated process, and in knee replacement surgery, the blood inflammatory response and thrombosis are inevitable and controversial issues. Many factors affect the expression of inflammatory factors during surgery, such as the surgical operation, time, instruments, and even anaesthesia. However, these factors should be considered in future studies. However, the existing evidence needs to be further expanded. The current conclusions only simulated a model of unilateral preliminary knee replacement and did not address knee revision or bilateral knee replacement surgery. One study found that low-molecular-weight heparin inhibits neutrophil adhesion to activated endothelial cells by binding to P-selectin [[33]]. The use of heparin can mediate anti-inflammatory effects by inhibiting the pathway of the nuclear inflammatory transcription factor NF- κ B [[34]].

We will continue investigating whether ES-PMMA bone cement affects inflammatory factors, such as IL-1 β , IL-8, and IL-17, in future studies. In particular, we will investigate the NF- κ B signalling pathway and the mechanisms involved in leukocyte and endothelial cell adhesion by binding to P/L-selectin. In this context, the role of ES-PMMA in promoting osteogenesis by inhibiting the local inflammatory response also requires further research.

5. Conclusion

The addition of the anticoagulant enoxaparin sodium to PMMA bone cement was found to produce a local anti-inflammatory effect with significant advantages over conventional PMMA bone cement. More importantly, we found that this novel material could reduce the rate of local endothelial cell apoptosis and decrease endothelial cell damage by regulating the expression of inflammatory factors IL-6 and TNF- α .

Funding

The authors thank Professor Dehao Fu for his guidance, as well as the support of the Local Science and Technology Development Fund Project (226Z7720G) and the Xinjiang Project.

Author contributions

Kangning Hao, Luobin Ding, and Linchao Sang contributed to the methodology, validation, and investigation. Kangning Hao and Xiaoyu Shen wrote the original draft, performed data curation, obtained resources, and conducted formal analysis. Xiangbei Qi and Dehao Fu performed conceptualization and wrote, reviewed, edited, and supervised the study. Xiangbei Qi was responsible for the project administration and funding.

Data availability statement

Data included in article/supp. material/referenced in article.

Ethics approval and consent to participate

All experiments were approved by the Animal Experimentation Ethics Committee of the Third Hospital of Hebei Medical University (z2021-007-2). All experiments were performed in strict accordance with the guidelines for the care and use of laboratory animals, and the study was performed in compliance with the ARRIVE guidelines.

Consent for publication

Not applicable.

Availability of data and materials

The data associated with the paper can be accessed from the corresponding author.

Declaration of competing interest

No potential conflict of interest was reported by the authors.

Acknowledgments

Not applicable.

Appendix A. Supplementary data

Supplementary data to this article can be found online at <https://doi.org/10.1016/j.heliyon.2023.e16530>.

References

- [1] S. Gao, X. Qi, J. Li, L. Sang, Upregulated KAT7 in synovial fibroblasts promotes Th17 cell differentiation and infiltration in rheumatoid arthritis, *Biochem. Biophys. Res. Commun.* 489 (2017) 235–241, <https://doi.org/10.1016/j.bbrc.2017.05.143>.
- [2] C. Aubrun-Fillâtre, F. Monchau, P. Hivart, Acrylic bone cement, and starch: botanical variety impact on curing parameters and degradability, *Mater. Sci. Eng. C* 69 (2016) 1328–1334, <https://doi.org/10.1016/j.msec.2016.08.023>.
- [3] M.A. Rothermich, J.M. Buchowski, D.B. Bumpass, et al., Pulmonary cement embolization after vertebroplasty requiring pulmonary wedge resection, *Clin. Orthop. Relat. Res.* 472 (2014) 1652–1657, <https://doi.org/10.1007/s11999-014-3506-0>.
- [4] N.A. Lamparello, V. Jaswani, K. DeSousa, et al., Percutaneous retrieval of an embolized kyphoplasty cement fragment from the pulmonary artery: a case report and literature review, *J. Radiol. Case Rep.* 10 (2016), <https://doi.org/10.3941/jrcr.v10i7.2806>.
- [5] A.S. Barakat, T. Owais, M. Alhashash, et al., Presentation and management of symptomatic central bone cement embolization, *Eur. Spine J.* 27 (2017) 2584–2592, <https://doi.org/10.1007/s00586-017-5267-4>.
- [6] H. Sun, X. Ma, Z. Li, J. Liu, et al., Release characteristics of enoxaparin sodium-loaded polymethylmethacrylate bone cement, *J. Orthop. Surg. Res.* 16 (2021), <https://doi.org/10.1186/s13018-021-02223-w>.
- [7] L. Sang, K. Hao, L. Ding, X. Shen, H. et al., The mechanism by which enoxaparin sodium–high-viscosity bone cement reduces thrombosis by regulating CD40 expression in endothelial cells, *BMC Musculoskel. Disord.* 23 (2022), <https://doi.org/10.1186/s12891-022-05469-5>.
- [8] Zhihang Xiao, Dehao Fu, Li Zhang, et al., Bone healing study of alendronate combined with enoxaparin sodium bone cement in rabbits with bone defects, *J. Orthop. Surg. Res.* 17 (1) (2022) 431, <https://doi.org/10.1186/s13018-022-03330-y>.
- [9] C.E. Heim, K.J. Yamada, R. Fallet, J. Odvody, et al., Orthopaedic surgery elicits a systemic anti-inflammatory signature, *J. Clin. Med.* 9 (2020) 2123, <https://doi.org/10.3390/jcm9072123>.
- [10] E. Rawish, H. Nording, T. Münte, H.F. Langer, Platelets as mediators of neuroinflammation and thrombosis, *Front. Immunol.* 11 (2020), 548631, <https://doi.org/10.3389/fimmu.2020.548631>.
- [11] Q. Pan, C. Zhang, X. Wu, Y. Chen, Identification of a heparosan heptasaccharide as an effective anti-inflammatory agent by partial desulfation of low molecular weight heparin, *Carbohydr. Polym.* 227 (2020), 115312, <https://doi.org/10.1016/j.carbpol.2019.115312>.
- [12] Z. Franks, R.A. Campbell, A. Vieira de Abreu, J.T. Holloway, J.E. Marvin, B.F. Kraemer, et al., Methicillin-resistant *Staphylococcus aureus*-induced thrombo-inflammatory response is reduced with timely antibiotic administration, *Thromb. Haemostasis* 109 (2013) 684–695, <https://doi.org/10.1160/TH12-08-0543>.
- [13] X. Chen, R. Han, P. Hao, L. Wang, M. Liu, M. Jin, et al., Nepetin inhibits IL-1 β induced inflammation via NF- κ B and MAPKs signaling pathways in ARPE-19 cells, *Biomed. Pharmacother.* 101 (2018) 87–93, <https://doi.org/10.1016/j.biopha.2018.02.054>.
- [14] Jianhua Liu, Dongliang Xu, Shiming Yu, Junyong Hu, et al., The effect of tranexamic acid on occult blood loss in an animal model of total knee replacement[J], *Chin. J. Reconstruct. Surg.* 23 (4) (2009) 463–467, <http://www.hxyx.com/article/zgxfjwkzz/2009/4/463>.
- [15] Y. lei, N. Bao, J. Zhao, Effects of tranexamic acid on hidden blood loss after total knee arthroplasty in animal models 19 (17) (2015) 2648–2654, <https://www.cjter.com/CN/10.3969/j.issn.2095-4344.2015.17.005>.
- [16] M.K. Wasko, M. Struminski, K. Bobecka-Wesolowska, J. Kowalczewski, Neutrophil-to-lymphocyte ratio shows faster-changing kinetics than C-reactive protein after total hip and knee arthroplasty, *J. Orthop. Trans.* 10 (2017) 36–41, <https://doi.org/10.1016/j.jot.2017.05.008>.
- [17] H.J.C. Kluijn-Nelemans, K. Meijer, Y.I.G.V. Tichelaar, Infections and inflammatory diseases as risk factors for venous thrombosis, *Thromb. Haemostasis* 107 (2012) 827–837, <https://doi.org/10.1160/th11-09-0611>.
- [18] A. Langkilde, T.L. Jakobsen, T.Q. Bandholm, J. Eugen-Olsen, et al., Inflammation and postoperative recovery in patients undergoing total knee arthroplasty—secondary analysis of a randomized controlled trial, *Osteoarthritis Cartilage* 25 (2017) 1265–1273, <https://doi.org/10.1016/j.joca.2017.03.008>.
- [19] B. Cusack, D.J. Buggy, Anaesthesia, analgesia, and the surgical stress response, *BJA Educ.* 20 (2020) 321–328, <https://doi.org/10.1016/j.bjae.2020.04.006>.
- [20] T. Wu, S. He, Z. Jiao, X. Liang, et al., Low molecular weight heparin improves the inflammatory state of acute sinusitis rats through inhibiting the TLR4-MyD88-NF- κ B signaling pathway, *Front. Pharmacol.* 12 (2021), <https://doi.org/10.3389/fphar.2021.726630>.
- [21] C. Bal dit Sollier, J.-G. Dillinger, L. Drouet, Anticoagulant activity and pleiotropic effects of heparin, *JMV-Journal de Médecine Vasculaire* 45 (2020) 147–157, <https://doi.org/10.1016/j.jdmv.2020.03.002>.
- [22] J. Choi, S. Moon, H. Bae, Y.-W. Kim, Y. Seo, et al., Anti-inflammatory effects of alnus Sibirica extract on in vitro and in vivo models, *Molecules* 25 (2020) 1418, <https://doi.org/10.3390/molecules25061418>.
- [23] E.-N. Kim, T.-Y. Kim, E.K. Park, J.-Y. Kim, G.-S. Jeong, Panax ginseng fruit has anti-inflammatory effect and induces osteogenic differentiation by regulating Nrf2/HO-1 signaling pathway in in vitro and in vivo models of periodontitis, *Antioxidants* 9 (2020) 1221, <https://doi.org/10.3390/antiox9121221>.
- [24] L. B, D.G. Feng, F. Wang, J.X. Wang, C.G. Xu, MiR-365 participates in coronary atherosclerosis through regulating IL-6, *Eur. Rev.* 20 (24) (2016) 5186–5519, <https://www.europearreview.org/article/11930>.
- [25] S.J. Ha, J. Lee, K.-M. Song, Y.H. Kim, N.H. Lee, Y.-E. Kim, S.K. Jung, Ultrasonicated *Lеспедеза* cuneata extract prevents TNF- α -induced early atherosclerosis in vitro and in vivo, *Food Funct.* 9 (2018) 2090–2101, <https://doi.org/10.1039/c7fo01666b>.
- [26] M.L. Valle, J. Dworschak, A. Sharma, A.S. Ibrahim, et al., Inhibition of interleukin-6 trans-signaling prevents inflammation and endothelial barrier disruption in retinal endothelial cells, *Exp. Eye Res.* 178 (2019) 27–36, <https://doi.org/10.1016/j.exer.2018.09.009>.
- [27] K. Shirakura, R. Ishiba, T. Kashio, M. Sakai, et al., Endothelial Robo4 regulates IL-6 production by endothelial cells and monocytes via a crosstalk mechanism in inflammation, *Biochem. Biophys. Res. Commun.* 495 (2018) 801–806, <https://doi.org/10.1016/j.bbrc.2017.11.067>.
- [28] H. Zhang, Y. Park, J. Wu, X. Ping Chen, S. et al., Role of TNF- α in vascular dysfunction, *Clin. Sci.* 116 (2009) 219–230, <https://doi.org/10.1042/cs20080196>.
- [29] B. Marcos-Ramiro, D. Garcia-Weber, J. Millán, TNF-induced endothelial barrier disruption: beyond actin and Rho, *Thromb. Haemostasis* 112 (2014) 1088–1102, <https://doi.org/10.1160/th14-04-0299>.
- [30] P. Nallasamy, Z.Y. Kang, X. Sun, P.V. Anandh Babu, D. Liu, Z. Jia, Natural compound resveratrol attenuates TNF-Alpha-Induced vascular dysfunction in mice and human endothelial cells: the involvement of the NF- κ B signaling pathway, *Int. J. Mol. Sci.* 22 (2021), 12486, <https://doi.org/10.3390/ijms222112486>.

- [31] W.-P. Kao, C.-Y. Yang, T.-W. Su, Y. T, et al., The versatile roles of CARDs in regulating apoptosis, inflammation, and NF- κ B signaling, *Apoptosis* 20 (2014) 174–195, <https://doi.org/10.1007/s10495-014-1062-4>.
- [32] T.W. Jung, H.S. Park, G.H. Choi, et al., β -aminoisobutyric acid attenuates LPS-induced inflammation and insulin resistance in adipocytes through AMPK-mediated pathway, *J. Biomed. Sci.* 25 (2018), <https://doi.org/10.1186/s12929-018-0431-7>.
- [33] C. Shi, W. Tingting, J.P. Li, M.A. Sullivan, et al., Comprehensive landscape of heparin therapy for COVID-19, *Carbohydr. Polym.* 254 (2021), 117232, <https://doi.org/10.1016/j.carbpol.2020.117232>.
- [34] C. Bal Dit Sollier, J.G. Dillinger, L. Drouet, Anticoagulant activity and pleiotropic effects of heparin, *J. Med. Vasc.* 45 (3) (2020) 147–157, <https://doi.org/10.1016/j.jdmv.2020.03.002>.